Epilepsy Research (2010) 89, 303–309

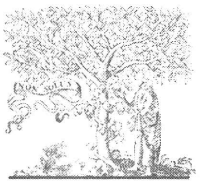

journal homepage: www.elsevier.com/locate/epilepsyres

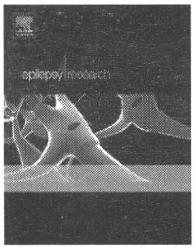

Genomic copy number variations at 17p13.3 and epileptogenesis

Keiko Shimojima[a], Chitose Sugiura[b], Hiroka Takahashi[c], Mariko Ikegami[c], Yukitoshi Takahashi[c], Kousaku Ohno[b], Mari Matsuo[d], Kayoko Saito[d], Toshiyuki Yamamoto[a,*]

[a] *International Research and Educational Institute for Integrated Medical Sciences (IREIIMS), Tokyo Women's Medical University, Tokyo, Japan*
[b] *Division of Child Neurology, Institute of Neurological Science, Faculty of Medicine, Tottori University, Yonago, Japan*
[c] *National Epilepsy Center, Shizuoka Institute of Epilepsy and Neurological Disorders, Shizuoka, Japan*
[d] *Institute of Medical Genetics, Tokyo Women's Medical University, Tokyo, Japan*

Received 9 December 2009; received in revised form 4 February 2010; accepted 11 February 2010
Available online 12 March 2010

KEYWORDS
17p13.3;
Array comparative genomic hybridization (array CGH);
LIS1;
YWHAE;
Fluorescent *in situ* hybridization (FISH);
Epileptogenesis

Summary Deletion of the terminal end of 17p is responsible for Miller-Dieker syndrome (MDS), which is characterized by lissencephaly, distinctive facial features, growth deficiency, and intractable seizures. Using microarray-based comparative genomic hybridization, 3 patients with epilepsy were revealed to have genomic copy number aberrations at 17p13.3: a partial *LIS1* deletion in a patient with isolated lissencephaly and epilepsy, a triplication of LIS1 in a patient with symptomatic West syndrome, and a terminal deletion of 17p including *YWHAE* and *CRK* but not *LIS1* in a patient with intractable epilepsy associated with distinctive facial features and growth retardation. In this study, it was suggested that the identified gain or loss of genomic copy numbers within 17p13.3 result in epileptogenesis and that triplication of *LIS1* can cause symptomatic West syndrome.

Introduction

The terminal end of the short arm of chromosome 17 is crucial for neurodevelopment and deletion of this region is associated with Miller-Dieker syndrome (MDS), a congenital malformation syndrome consisting of typical lissencephaly and distinctive facial features. Patients with MDS also show growth deficiency, severe developmental delays, and intractable seizures (Dobyns et al., 1991). MDS results from chromosomal disruption, including cytogenetically visible or submicroscopic deletions of the 17p13.3 region, which includes *LIS1*, a key indicator of MDS (Dobyns et al., 1993; Reiner et al., 1993). *LIS1* encodes PAFAH1B1 and participates in neural migration, disruption of which is responsible for lissencephaly. Indepen-

* Corresponding author at: International Research and Educational Institute for Integrated Medical Sciences (IREIIMS), Tokyo Women's Medical University, 8-1 Kawada-cho, Shinjuku-ward, Tokyo 162-8666, Japan. Tel.: +81 3 3353 8111x24067; fax: +81 3 3352 3088.
E-mail address: yamamoto@imcir.twmu.ac.jp (T. Yamamoto).

0920-1211/$ – see front matter © 2010 Elsevier B.V. All rights reserved.
doi:10.1016/j.eplepsyres.2010.02.002

dent *LIS1* deletions or nucleotide alterations in its coding exons cause isolated lissencephaly without growth deficiency or distinctive facial features (Cardoso et al., 2000). This finding indicates that the clinical manifestations associated with MDS patients, such as growth deficiency and dysmorphic features, are likely derived from other genes included in the 17p13.3 region. Genotype–phenotype correlation studies in patients with deletions in the terminal region of 17p revealed that *LIS1* deletion is responsible for lissencephaly and that combined deletion of *LIS1* and *YWHAE* results in severer lissencephaly and a distinctive facial appearance, the hallmarks of MDS (Cardoso et al., 2003).

Recent revolutionary technological advances in molecular cytogenetics have enabled us to identify submicroscopic chromosomal abnormalities including gain or loss of genomic copy numbers (Emanuel and Saitta, 2007). Such genomic copy number variations (CNV) have only recently been identified using microarray-based comparative genomic hybridization (aCGH), and the incidence of such abnormalities seems to be more frequent than was thought prior to the human genome project (Shaffer et al., 2007). Genomic duplications are of particular interest because many submicroscopic duplications have been shown to be related to neurological disorders, including developmental delay and epilepsy (Lee and Lupski, 2006). Small genomic deletions and duplications have also been reported in 17p13.3 (Bi et al., 2009; Haverfield et al., 2009; Mei et al., 2008; Mignon-Ravix et al., 2009; Roos et al., 2009; Sreenath Nagamani et al., 2009).

In this study, we identified three types of genomic CNVs in the chromosome 17p13.3 region in 3 patients with epilepsy. This result implicates the dose effects of the genes in the 17p terminal region in epilepsy.

Materials

After obtaining informed consents from the patients' families based on the permission approved by the ethical committee of the institution, peripheral blood samples were obtained from 300 patients with psychomotor developmental delay and/or epilepsy, which included 10 patients with early infantile epileptic encephalopathy, 43 patients with West syndrome, 2 patients with Lennox-Gastaut syndrome, 12 patients with symptomatic generalized epilepsy, 14 patients with symptomatic partial epilepsy, and 5 patients with other types of epilepsy.

Methods

aCGH analysis was performed using the Human Genome CGH Microarray 105A chip (Agilent Technologies, Palo Alto, CA, USA), according to the manufacturer's protocol (Shimojima et al., 2009). Genomic DNAs were extracted from peripheral blood using a QIAquick DNA extraction kit (Qiagen, Hilden, Germany), and genomic copy numbers were determined using CGH Analytics software version 3.5 (Agilent Technologies).

To confirm the genomic copy number variations identified by aCGH, fluorescent *in situ* hybridization (FISH) analysis was performed as described (Shimojima et al., 2009). To confirm whether the identified genomic copy number variations were de novo or not, parental samples were also obtained and analyzed.

The wild-type genomic sequence of *LIS1* exons 9–11 was amplified by long PCR using LA-Taq (Takara, Otsu, Japan), a forward primer designed to anneal within intron 8 (5′-CAGTGCTGTGCTATAACTGCACTATC-3′), and a reverse primer designed to anneal within exon 9 (5′-CACTGGCAGGTGTATACTATCAGATAC-3′), according to the manual provided by the manufacture. Then, the 2867-bp amplicon was cloned into the p-GEM T-vector® (Promega, Madison, WI, USA), and the resulting plasmid was used as a probe for FISH analysis. The bacterial artificial chromosome (BAC) clones mapped to chromosome 17p13.3 (Table 1) were selected from an in silico library (UCSC Human Genome Browser, March 2006, http://genome.ucsc.edu).

Fiber-FISH analysis was performed to determine the directionality of the repeated segments as described elsewhere (Shimojima et al., 2009).

Results

Molecular and cytogenetic analysis

In patient 1, a loss of genomic copy number was identified by aCGH. The deletion was comprised of a 294-kb region of chr17 (2,522,672–2,816,939), including the last 5 exons of *LIS1* (exons 7–11) and the neighboring *KIAA0664* and *GARNL* (Fig. 1). FISH analysis using an originally cloned plasmid probe containing the predicted deletion sequence confirmed the deletion of one copy of *LIS1* (Fig. 2A). The fact that neither parent had the *LIS1* deletion (data not shown) confirmed it as a de novo deletion in patient 1.

Table 1 Summary of FISH analyses.

Clone	Band	Start[a]	End[a]	Patient 1	Patient 2	Patient 3	Coverage genes
RP11-629C16	17p13.3	373,082	560,333	NT	NT	Deletion	
RP11-356I18	17p13.3	707,755	880,135	NT	NT	Deletion	
RP11-294J5	17p13.3	1,146,211	1,299,309	NT	NT	Deletion	*YWHAE, CRK*
RP11-380H7	17p13.3	2,026,967	2,250,500	NT	Duplication	NT	
RP11-135N5	17p13.3	2,312,022	2,492,178	NT	Triplication	NT	*LIS1*
CTD-2576K4	17p13.3	2,492,176	2,643,505	NT	Triplication	NT	*LIS1*
Plasmid[b]	17p13.3	2,528,949	2,530,730	Deletion	NT	NT	*LIS1*
RP11-1D5	17p13.1	7,918,567	8,082,208	Marker	Marker	NT	
RP11-153A23	17q25.3	73,516,547	73,694,284	NT	NT	Marker	

NT: not tested.

[a] Genomic position is according to the May 2006 human reference sequence (Build 2006).

[b] Originally constructed plasmid probe.

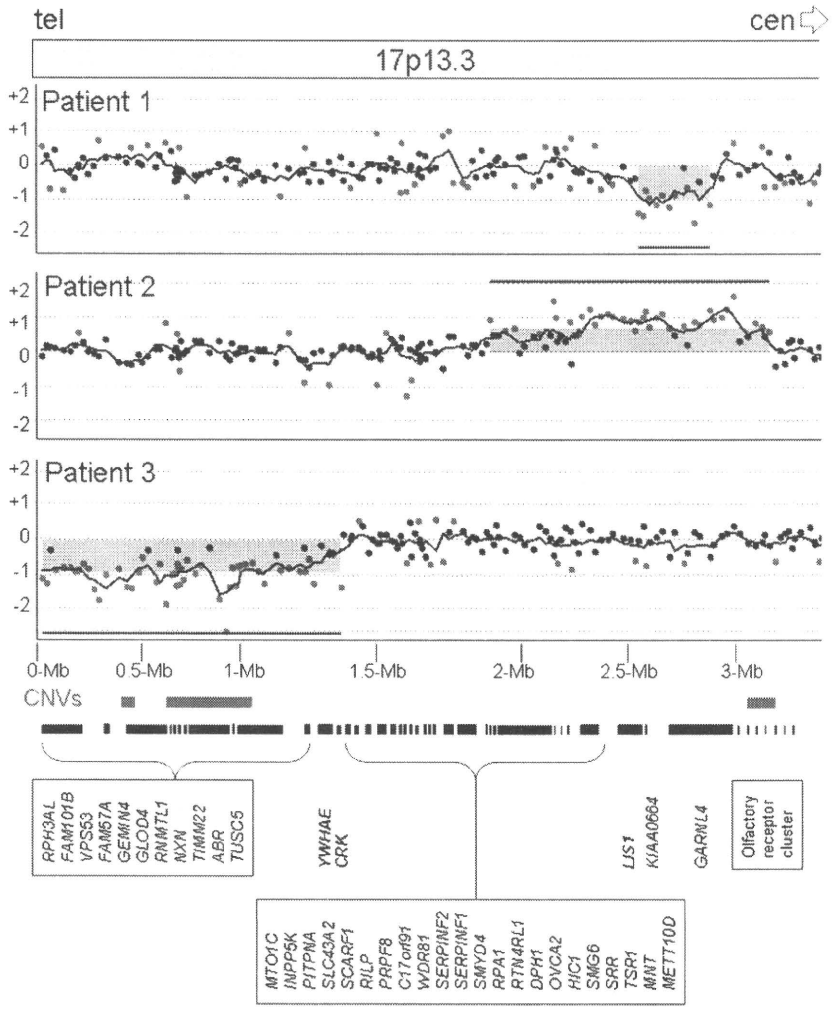

Figure 1 aCGH analysis of the 17p13.3 region in 3 epilepsy patients and a corresponding genetic map of the MDS region. Genomic copy number aberrations were identified in 3 patients by CGH Analytics software. The horizontal and vertical axes indicate the position along 17p13.3 and the $\log_2$ ratio of the genomic copy number, respectively. The gray rectangles indicate regions of copy number aberrations. The dots indicate the annealing locations and the corresponding $\log_2$ ratios for each probe. The black dots indicate normal $\log_2$ ratio; whereas, red and green indicate $\log_2$ ratio higher than 0.5 and lower than −0.5, respectively. The red and black rectangles indicate locations of the previously reported CNVs and the known genes in the indicated regions. The names of the known genes are indicated below the figure, and *YWHAE*, *CRK*, and *LIS1* are highlighted in bold. (For interpretation of the references to color in this figure caption, the reader is referred to the web version of the article.)

In patient 2, a gain of genomic copy number was identified by aCGH in the MDS region containing *LIS1* (Fig. 1). The mean $\log_2$ signal ratios were +0.5 in chr17 (1,899,328–2,151,328) and +1 in chr17 (2,165,727–3,065,623), indicating duplication and triplication, respectively. These aberrations were confirmed by FISH analysis (Fig. 2B and Table 1), and fiber-FISH analyses revealed the directions of all triplicated segments with tandem insertions (Fig. 2D). The fact that neither parent of patient 2 showed any signal abnormalities in FISH analysis (data not shown) confirmed the de novo triplication in patient 2.

In patient 3, aCGH analysis revealed a terminal deletion of 17p, chr17 (1–1,280,058), which included *YWHAE* and *CRK*, but not *LIS1* (Fig. 1). This was confirmed by FISH analysis (Fig. 2C). The parental samples showed no abnormalities in this region (data not shown), indicating de novo deletion of 17p in patient 3.

Clinical reports

Patient 1 is a 22-year-old female was born at 38 gestational weeks with a weight of 2540 g (<25th centile). Since the patient showed no eye following and no responsive smiles at the age of 5 months, she was admitted to the hospital, and global agyria was identified by brain computed tomography (CT). In infancy, she started to suffer from several types of seizures, most of which were generalized tonic–clonic seizures, and an electroencephalography (EEG) examination showed irregular high-voltage slow waves with continuous multi-focal sharp waves (data not shown). These epileptic seizures were refractory to medical treatment. At the age of 16 years and 7 months, brain magnetic resonance imaging (MRI) analysis revealed lissencephaly with a predominance in the posterior region indicating grade 3 lissencephaly (Fig. 3A–C) (Kato and Dobyns, 2003). She

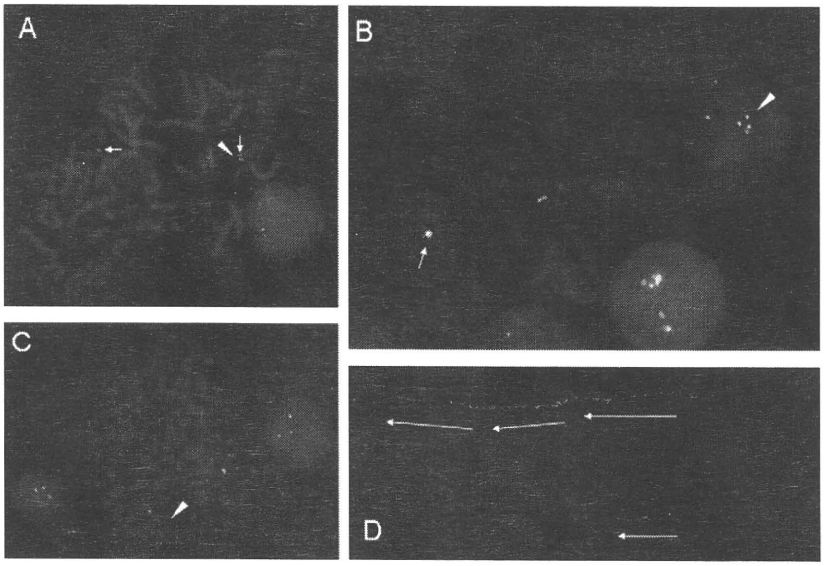

Figure 2 FISH and fiber-FISH analysis of the 3 patients. (A) Patient 1: partial deletion of *LIS1* was identified. The arrows indicate markers of chromosome 17 (RP11-1D5; red), and the arrowhead indicates the originally constructed partial sequence of *LIS1* (green). (B) Patient 2: duplication of *LIS1* was identified. FISH analysis indicated a predominant *LIS1* signal (RP11-135N5; green) in one allele of chromosome 17 (arrow) and increased *LIS1* signal numbers in metaphase (arrowhead). The red signals indicate markers, RP11-1D5. (C) Patient 3: one allele of *YWHAE* (RP11-356I18; green) is deleted (arrowhead). The red signals indicate markers, RP11-153A23. (D) Patient 2: fiber-FISH analysis identified a tandem triplication of the *LIS1* region in one of the chromosomal fibers. The green signals represent RP11-135N5, and the red signals represent CTD-2576K4. The arrows reflect a single unit of *LIS1* staining. The single arrow at the bottom represents a normal chromosome 17. (For interpretation of the references to color in this figure caption, the reader is referred to the web version of the article.)

was diagnosed with isolated lissencephaly because of her normal facial features (Fig. 4A). At 22 years of age, she showed good eye contact, visual tracking, social smiling, and various other facial expressions in response to parental vocalization, although she could not speak and had no head control. Epileptic seizures occurred several times a week. She was capable of taking oral paste foods and did not need tube feeding at home. Conventional G-banding chromosomal analysis showed a normal female karyotype (46,XX), and subsequent FISH analysis using a commercially available

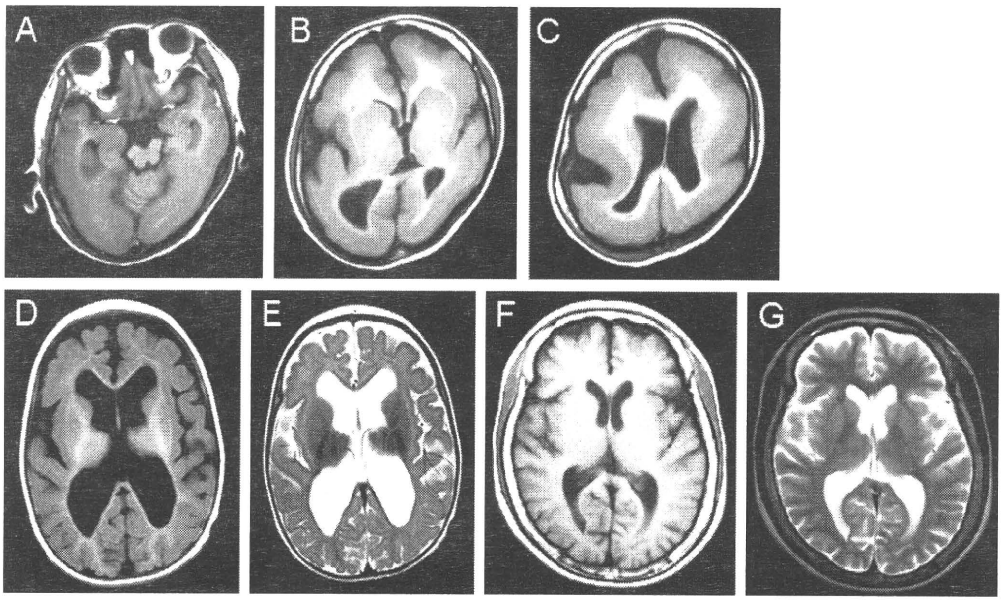

Figure 3 Brain MRI images of the three patients. (A–C) Grade 3 lissencephaly with predominant agyria in the posterior region was seen in patient 1. (D and E) Generalized hypoplasia of the brain involving the cortical and white matter regions was noted in patient 2. (F and G) Mild volume loss of the brain was identified in patient 3. (A–D, F) T1-weighted MRI image. (E and G) T2-weighted MRI image.

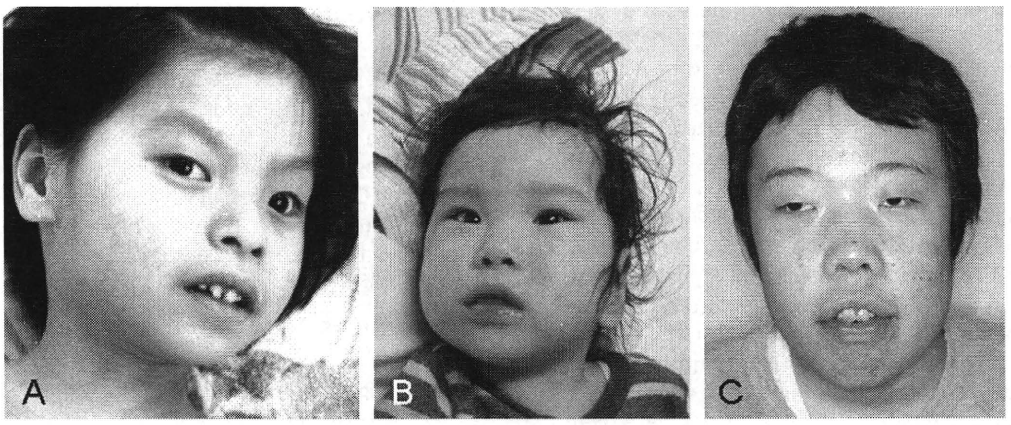

Figure 4 Portraits of the three patients. There were no distinct facial morphologies for patient 1 (A) or patient 2 (B). (C) Patient 3 showed a prominent forehead, bilateral ptosis, a broad nasal root, epicanthal folds, and retrognathia. Signed consent forms authorizing publication of the unmasked images of all identifiable patients have been obtained from the patients and/or their guardians.

probe, the Vysis Miller-Dieker Region/Isolated Lissencephaly Probe LSI *LIS1* (Abbott Laboratories, Abbott Park, IL, USA), indicated no deletion at 17p13.3 (data not shown).

Patient 2 is an 11-month-old girl was referred to us for infantile spasms. She was born at 39 weeks gestation with a birth weight of 1992 g (<3rd centile). At 6 months, her first epileptic seizure with deviation of eye position was noted, and EEG analysis showed modified hypsarrhythmia with synchronized high-voltage slow waves indicating West syndrome (Fig. 5). A subsequent brain MRI examination revealed generalized hypoplasia of the brain involving the cortical and white matter regions, associated with hypoplasia of the corpus callosum, which resulted in ventricular dilatation (Fig. 3C). Although several orally administered anti-epileptic drugs were ineffective, subsequent adrenocorticotropic hormone (ACTH) therapy was effective. At 6 months, she lacked neck control and could not roll over due to severe hypotonia. Conventional G-banding showed a normal female karyotype. At the age of 21 months, patient 2 showed an average growth rate with her length of 83.5 cm (=50th centile), weight of 10.0 kg (=50th centile), and head circumference of 47.0 cm (=50th centile). At this time, she was able to turn over but could not sit alone, indicating a severe developmental delay.

Patient 3 is a 23-year-old male was born to healthy parents at 39 weeks gestation with a birth weight of 2500 g (<50th centile). Delivery was uneventful. He suffered from mild developmental delay in infancy and from secondary generalized partial seizures at the age of 6 years. Subsequently, he suffered various types of seizures that were refractory to many different anti-epileptic drugs. Communication was challenging for him. At the age of 20 years, the Wechsler Adult Intelligence Scale (WAIS) indicated that his full IQ was 45 (verbal = 59, performance = 45). At the time of the study, he was working at a social welfare institution. His height was 155.5 cm (<3rd centile), his weight was 52.3 kg (<25th centile), and his head circumference was 56.2 cm (<25th centile). He had distinctive facial features (Fig. 4C). Conventional G-banding showed a normal male karyotype of 46,XY. A brain MRI examination revealed mild volume loss of the brain (Fig. 3F and G).

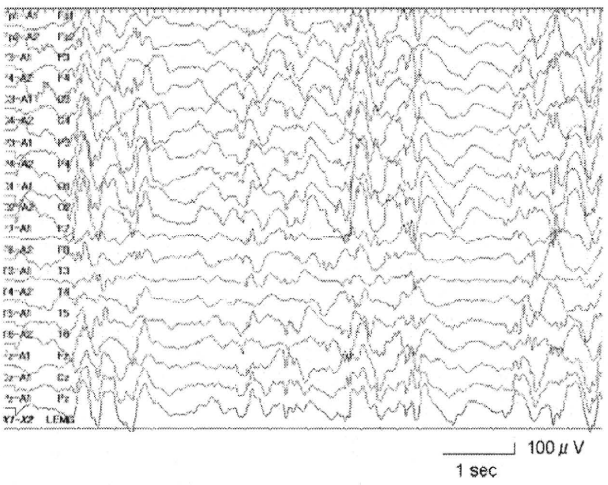

Figure 5 EEG analysis of patient 2, indicating modified hypsarrhythmia.

Discussion

In this study, we identified pathogenic CNVs in 17p13.3, the MDS critical region, in 3 epileptic patients.

Patient 1 had isolated grade 3 lissencephaly (Kato and Dobyns, 2003) but lacked the dysmorphic features common among MDS patients. As a commercially available *LIS1* probe did not detect deletion, aCGH analysis was performed and identified a microdeletion involving the last 5 exons of *LIS1*. This was similar to the findings of the previous report, in which FISH analysis using a commercially available *LIS1* probe yielded a false-negative result for a patient with a deletion in the 5′ region of *LIS1* (Izumi et al., 2007). In both cases, the incorrect analysis resulted from a partial *LIS1* deletion and from the limited availability of commercial FISH analysis probes. The deletion region of patient 1 included two other neighboring genes; *KIAA0664*, which encodes a hypothetical protein, and *GARNL4*, which encodes a GTPase-activating protein that activates the small guanine-nucleotide-binding protein Rap1 in platelets. Thus,

their detailed functions in the central nervous system are unknown. Patient 1 has shown long-term survival without physical or mental deterioration despite the fact that the majority of patients with lissencephaly die early in childhood (de Rijk-van Andel et al., 1990). In contrast, MDS patients with a large telomeric deletion of 17p13.3 present with a severe phenotype, including lissencephaly; significant facial dysmorphism; and occasionally other congenital visceral anomalies such as gastrointestinal and cardiac defects; and furthermore, the severity of lissencephaly in MDS patients is severer than that seen in cases of isolated lissencephaly (Cardoso et al., 2003; Dobyns et al., 1991).

Mei et al. (2008) analyzed 45 patients with isolated lissencephaly; 44% of the patients (20/45) showed *LIS1* mutations, and small deletions/duplications were identified in 76% of the patients without *LIS1* mutations (19/25). One of the 19 patients lacking *LIS1* mutations exhibited duplication of three *LIS1* exons. Haverfield et al. (2009) analyzed 52 patients with lissencephaly, and intragenic duplication of *LIS1* was identified in 6 patients. These microduplications will disrupt *LIS1* structures and result in loss of function of the *LIS1* product. On the other hand, two recent reports described microduplications encompassing the entire *LIS1* region 11,13 (Bi et al., 2009; Roos et al., 2009). Using transgenic mice, Bi et al. (2009) confirmed that LIS1/PAFAH1B1 overexpression derived from genomic copy number gain was responsible for abnormal neurodevelopment. They also reported a patient with *LIS1* triplication (Subject 6) (Bi et al., 2009). Similarly, we identified a triplication of *LIS1* in patient 2, whose MRI demonstrated normal gyrus formation but a reduced cerebral volume. Patient 2 exhibited infantile spasms; whereas, the patient with *LIS1* triplication (Subject 6) reported by Bi et al. (2009) lacked seizure activity. This difference may have resulted from the size difference between them, as the triplication size of patient 2 was much larger than that of the patient (Subject 6) reported by Bi et al. (2009). Accordingly, genomic copy number aberrations at 17p13.3 including *LIS1* can lead to neurodevelopmental delay and epilepsy regardless of whether the aberration reflects a gain or loss of copy number.

In this study, patient 3 had a complete terminal deletion of 17p, and he demonstrated the dysmorphic facial features and growth retardation associated with mental retardation. This was compatible with a report by Sreenath Nagamani et al. (2009) in which haploinsufficiency of *YWHAE* and *CRK* was suggested to be responsible for facial dysmorphism and growth deficiency, respectively. However, in our present study, patient 3 had intractable epilepsy. Among the previously reported patients with a terminal deletion of 17p that did not include *LIS1*, only 1 patient with der(17)t(5;17)(p13.1;p13.3) was reported to have seizure episodes (Mutchinick et al., 1999).

In conclusion, it was suggested that the identified gain or loss of genomic copy number within 17p13.3 result in epileptogenesis and that triplication of *LIS1* can cause symptomatic West syndrome.

Conflict of interest

None of the authors has any conflict of interest to disclosure.

Acknowledgements

This work was supported by the International Research and Educational Institute for Integrated Medical Sciences and the Tokyo Women's Medical University, which is supported by the Program for Promoting the Establishment of Strategic Research Centers; Special Coordination Funds for Promoting Science and Technology; and Ministry of Education, Culture, Sports, Science and Technology (Japan).

References

Bi, W., Sapir, T., Shchelochkov, O.A., Zhang, F., Withers, M.A., Hunter, J.V., Levy, T., Shinder, V., Peiffer, D.A., Gunderson, K.L., Nezarati, M.M., Shotts, V.A., Amato, S.S., Savage, S.K., Harris, D.J., Day-Salvatore, D.L., Horner, M., Lu, X.Y., Sahoo, T., Yanagawa, Y., Beaudet, A.L., Cheung, S.W., Martinez, S., Lupski, J.R., Reiner, O., 2009. Increased LIS1 expression affects human and mouse brain development. Nat. Genet. 41, 168–177.

Cardoso, C., Leventer, R.J., Matsumoto, N., Kuc, J.A., Ramocki, M.B., Mewborn, S.K., Dudlicek, L.L., May, L.F., Mills, P.L., Das, S., Pilz, D.T., Dobyns, W.B., Ledbetter, D.H., 2000. The location and type of mutation predict malformation severity in isolated lissencephaly caused by abnormalities within the LIS1 gene. Hum. Mol. Genet. 9, 3019–3028.

Cardoso, C., Leventer, R.J., Ward, H.L., Toyo-Oka, K., Chung, J., Gross, A., Martin, C.L., Allanson, J., Pilz, D.T., Olney, A.H., Mutchinick, O.M., Hirotsune, S., Wynshaw-Boris, A., Dobyns, W.B., Ledbetter, D.H., 2003. Refinement of a 400-kb critical region allows genotypic differentiation between isolated lissencephaly. Miller-Dieker syndrome, and other phenotypes secondary to deletions of 17p13.3. Am. J. Hum. Genet. 72, 918–930.

de Rijk-van Andel, J.F., Arts, W.F., Barth, P.G., Loonen, M.C., 1990. Diagnostic features and clinical signs of 21 patients with lissencephaly type 1. Dev. Med. Child Neurol. 32, 707–717.

Dobyns, W.B., Curry, C.J., Hoyme, H.E., Turlington, L., Ledbetter, D.H., 1991. Clinical and molecular diagnosis of Miller-Dieker syndrome. Am. J. Hum. Genet. 48, 584–594.

Dobyns, W.B., Reiner, O., Carrozzo, R., Ledbetter, D.H., 1993. Lissencephaly. A human brain malformation associated with deletion of the LIS1 gene located at chromosome 17p13. JAMA 270, 2838–2842.

Emanuel, B.S., Saitta, S.C., 2007. From microscopes to microarrays: dissecting recurrent chromosomal rearrangements. Nat. Rev. Genet. 8, 869–883.

Haverfield, E.V., Whited, A.J., Petras, K.S., Dobyns, W.B., Das, S., 2009. Intragenic deletions and duplications of the LIS1 and DCX genes: a major disease-causing mechanism in lissencephaly and subcortical band heterotopia. Eur. J. Hum. Genet. 17, 911–918.

Izumi, K., Kuratsuji, G., Ikeda, K., Takahashi, T., Kosaki, K., 2007. Partial deletion of LIS1: a pitfall in molecular diagnosis of Miller-Dieker syndrome. Pediatr. Neurol. 36, 258–260.

Kato, M., Dobyns, W.B., 2003. Lissencephaly and the molecular basis of neuronal migration. Hum. Mol. Genet., 12 Spec No. 1, R89-96.

Lee, J.A., Lupski, J.R., 2006. Genomic rearrangements and gene copy-number alterations as a cause of nervous system disorders. Neuron 52, 103–121.

Mei, D., Lewis, R., Parrini, E., Lazarou, L.P., Marini, C., Pilz, D.T., Guerrini, R., 2008. High frequency of genomic deletions—and a duplication—in the LIS1 gene in lissencephaly: implications for molecular diagnosis. J. Med. Genet. 45, 355–361.

Mignon-Ravix, C., Cacciagli, P., El-Waly, B., Moncla, A., Milh, M., Girard, N., Chabrol, B., Philip, N., Villard, L., 2009. Deletion of YWHAE in a patient with periventricular heterotopias and marked corpus callosum hypoplasia. J. Med. Genet. 47, 132–136.

Mutchinick, O.M., Shaffer, L.G., Kashork, C.D., Cervantes, E.I., 1999. Miller-Dieker syndrome and trisomy 5p in a child carrying a derivative chromosome with a microdeletion in 17p13.3 telomeric to the LIS1 and the D17S379 loci. Am. J. Med. Genet. 85, 99–104.

Reiner, O., Carrozzo, R., Shen, Y., Wehnert, M., Faustinella, F., Dobyns, W.B., Caskey, C.T., Ledbetter, D.H., 1993. Isolation of a Miller-Dieker lissencephaly gene containing G protein beta-subunit-like repeats. Nature 364, 717–721.

Roos, L., Jonch, A.E., Kjaergaard, S., Taudorf, K., Simonsen, H., Hamborg-Petersen, B., Brondum-Nielsen, K., Kirchhoff, M., 2009. A new microduplication syndrome encompassing the region of the Miller-Dieker (17p13 deletion) syndrome. J. Med. Genet. 46, 703–710.

Shaffer, L.G., Theisen, A., Bejjani, B.A., Ballif, B.C., Aylsworth, A.S., Lim, C., McDonald, M., Ellison, J.W., Kostiner, D., Saitta, S., Shaikh, T., 2007. The discovery of microdeletion syndromes in the post-genomic era: review of the methodology and characterization of a new 1q41q42 microdeletion syndrome. Genet. Med. 9, 607–616.

Shimojima, K., Tanaka, K., Yamamoto, T., 2009. A de novo intrachromosomal tandem duplication at 22q13.1q13.31 including the Rubinstein-Taybi region but with no bipolar disorder. Am. J. Med. Genet. A 149A, 1359–1363.

Sreenath Nagamani, S.C., Zhang, F., Shchelochkov, O.A., Bi, W., Ou, Z., Scaglia, F., Probst, F.J., Shinawi, M., Eng, C., Hunter, J.V., Sparagana, S., Lagoe, E., Fong, C.T., Pearson, M., Doco-Fenzy, M., Landais, E., Mozelle, M., Chinault, A.C., Patel, A., Bacino, C.A., Sahoo, T., Kang, S.H., Cheung, S.W., Lupski, J.R., Stankiewicz, P., 2009. Microdeletions including YWHAE in the Miller-Dieker syndrome region on chromosome 17p13.3 result in facial dysmorphisms, growth restriction, and cognitive impairment. J. Med. Genet. 46, 825–833.

Jpn J Ophthalmol 2010;54:622–637

A Case of Fukuyama Congenital Muscular Dystrophy Associated with Negative Electroretinograms

Fukuyama congenital muscular dystrophy (FCMD) is a congenital dystrophy associated with brain and eye abnormalities.[1] FCMD is an autosomal recessive disorder and occurs only in Japanese. Common ocular findings are optic atrophy, high myopia, cataracts, and weakness of the orbicularis muscles.[1] Abnormal vascular anastomosis and avascularization in the peripheral retina have also been reported. The eyes are only occasionally affected severely, for example, with retinal detachment and microphthalmia.

It was originally believed that patients with FCMD had normal electroretinograms (ERGs),[2] although a slight reduction of the b-wave and reduced ERGs under photopic conditions have been reported.[3,4] We describe an infant with FCMD exhibiting a severe form of ocular phenotype and negative-type ERG under dark-adapted conditions, a finding that to our knowledge has not been reported before.

Case Report

A 1-year-old boy had appeared normal at birth except for a right eye that was slightly microphthalmic. When he was 1 month old, a diagnosis of retinal detachment was made for the right eye (Fig. 1). His left eye was myopic with a tigroid appearance over the entire retina with pallor of the optic disc. The retinal vessels were tortuous, and the temporal peripheral retina was avascularized in both eyes. A scleral encircling buckle and subsequent vitrectomies were used to repair the retinal detachment in the right eye, but the retina remained detached. Before the surgery, the level of creatinine kinase was elevated (3634 IU/l), and the pediatrician suspected congenital muscular dystrophy despite the lack of any distinctive signs or a family history of muscular dystrophy.

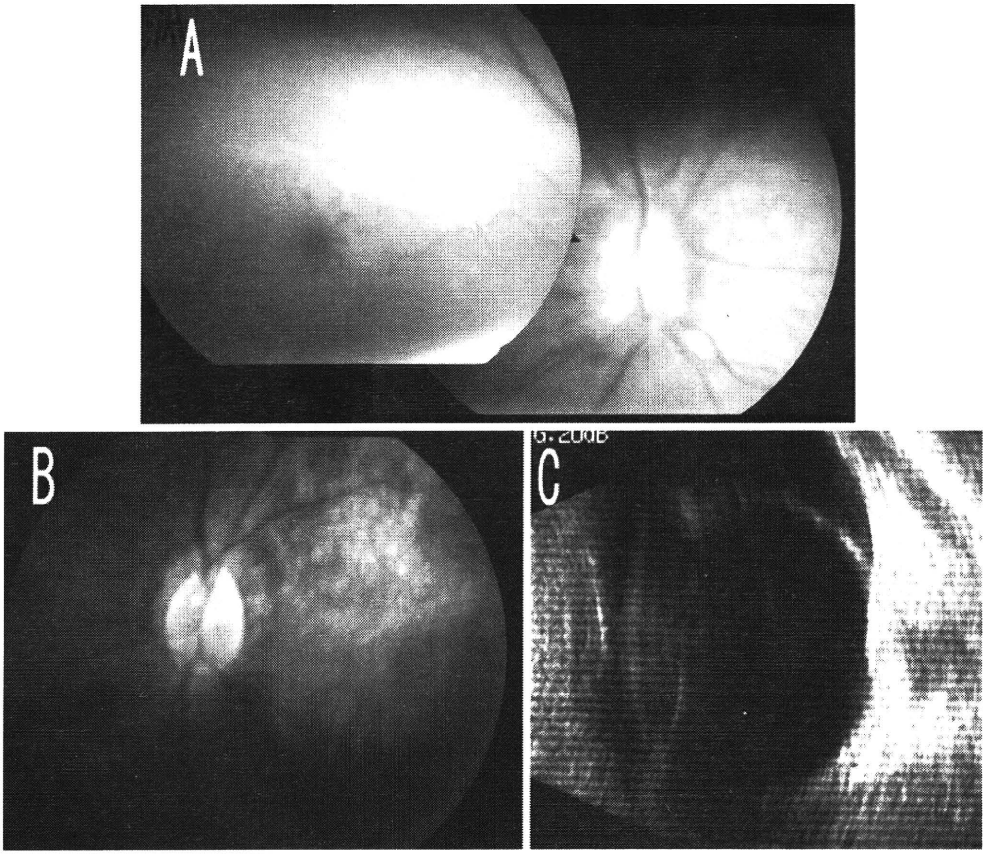

Figure 1A–C. Fundus photographs of our patient with Fukuyama congenital muscular dystrophy (FCMD). **A** Fundus photograph of the right eye showing a temporal retinal detachment involving the macula. **B** Fundus photograph of the left eye showing myopic tigroid appearance with pallor of the optic disc. **C** Ultrasonography showing the retinal detachment in the right eye.

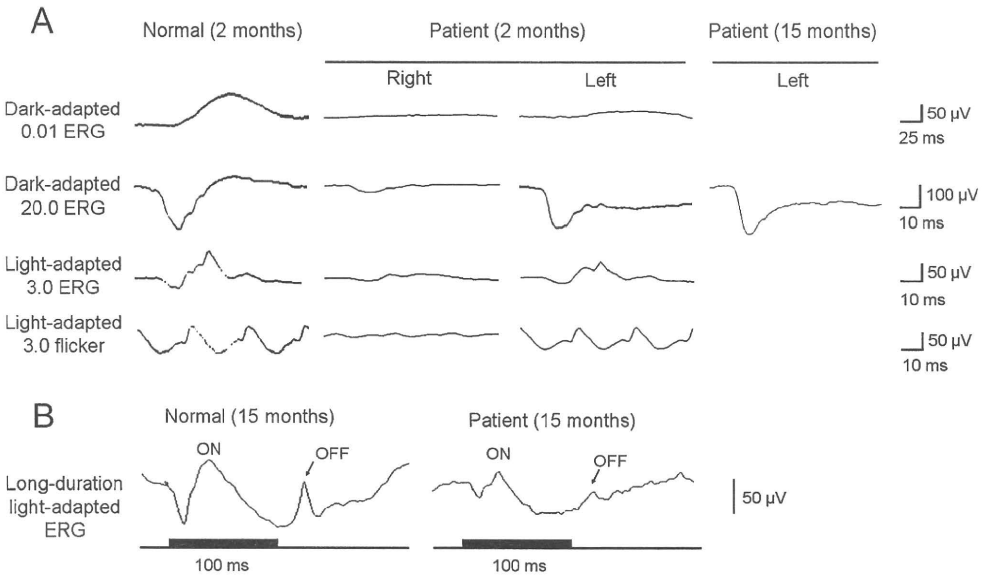

Figure 2A, B. Results of full-field electroretinograms (*ERGs*) using the International Society for Clinical Electrophysiology of Vision-recommended protocol recorded from our patient with FCMD. **A** ERGs recorded in a normal subject at age 2 months (left column), in our patient at 2 months (middle column), and in our patient at age 15 months. The amplitudes of the single-flash cone ERG and 30-Hz flicker ERGs were reduced but better preserved than the rod responses. Note that the maximum rod–cone response (dark-adapted, 20.0 ERG) of our patient showed a "negative" ERG waveform. **B** Light-adapted ERGs elicited by long-duration stimuli in a normal subject at age 15 months (*left*) and in our patient at age 15 months (*right*). Both the ON- and OFF-responses are equally reduced in our patient.

At 5 months, the patient was noted to have muscular weakness and was diagnosed with FCMD. The parents requested genetic testing to confirm the diagnosis. The patient was found to have compound heterozygous mutations in the *FKTN* gene; an insertion mutation in the 3′ noncoding region, and a point mutation, 250C- > T (R47X), in exon 3. The parents were found to be asymptomatic carriers.

During the first vitrectomy under general anesthesia, full-field ERGs were recorded using International Society for Clinical Electrophysiology of Vision-recommended standards (Fig. 2). Because of the retinal detachment, all ERG components in his right eye were severely attenuated. In his left eye, the rod response was decreased to about one-fifth of normal. The a-wave amplitude of the mixed rod–cone ERG was within normal limits, but the b-wave amplitude was smaller than the a-wave amplitude, indicating a negative-type ERG.

Comments

A negative ERG recorded under dark-adapted conditions has not been reported in patients with FCMD and therefore may be a new indication of FCMD. A compound heterozygous mutation in the *FKTN* gene, which occurs infrequently, is most likely the cause of the clinically severe phenotype. This negative-type ERG may be attributable to this less frequent genotype. A similar selective reduction of the b wave was described in patients with muscular dystrophies associated with changes in dystroglycan and dystrophin. The origin of the selective reduction is believed to be a disturbed neurotransmission from the photoreceptors to the ON-bipolar cells.[2]

To determine whether this negative-type ERG was caused by selective impairment of the postsynaptic ON-pathway, we also recorded light-adapted ERGs elicited by long-duration stimuli when our patient was 15 months old. We found that both the ON- and OFF-responses were equally reduced (Fig. 2B). This result is not in accord with the idea that the ON-bipolar cells are selectively disturbed, but an alternative possibility remains that the Müller cells or other neural elements are responsible for the reduction of the b wave because they are also believed to be involved in the generation of the b wave of ERGs.[5]

Acknowledgments. The authors thank Professor Akihiko Tawara for his critical comments and the patient and his parents for their cooperation. This work was partially supported by a Health and Labour Sciences Research Grant (20B-1) for Nervous and Mental Disorders and by Health and Labour Sciences Research Grants for Research on Intractable Diseases from the Ministry of Health, Labour and Welfare of Japan, and by Grants-in-Aid 19592047 and 22591956 for Scientific Research (C) from the Japan Society for the Promotion of Science.

Keywords: *FKTN*, Fukuyama congenital muscular dystrophy, microphthalmia, negative ERG, retinal detachment

Jpn J Ophthalmol
Vol 54: 622–637, 2010

Hiroyuki Kondo[1,2], Kayoko Saito[3], Mari Urano[3], Yukiko Sagara[3], Eiichi Uchio[2], and Mineo Kondo[4]
[1]Department of Ophthalmology, University of Occupational and Environmental Health, Japan, Kitakyushu, Japan; [2]Department of Ophthalmology, Fukuoka University School of Medicine, Fukuoka, Japan; [3]Institute of Medical Genetics, Tokyo Women's Medical University, Tokyo, Japan; [4]Department of Ophthalmology, Nagoya University Graduate School of Medicine, Nagoya, Japan

Received: February 24, 2010 / Accepted: June 29, 2010
Correspondence to: Hiroyuki Kondo, Department of Ophthalmology, University of Occupational and Environmental Health, Japan, 1-1 Iseigaoka, Yahatanishi-ku, Kitakyushu 807-8555, Japan
e-mail: kondohi@med.uoeh-u.ac.jp

DOI 10.1007/s10384-010-0875-0

References

1. Fukuyama Y, Osawa M, Suzuki H. Congenital progressive muscular dystrophy of the Fukuyama type—clinical, genetic and pathological considerations. Brain Dev 1981;3:1–29.
2. Santavuori P, Somer H, Sainio K, et al. Muscle-eye-brain disease (MEB). Brain Dev 1989;11:147–153.
3. Chijiiwa T, Nishimura M, Inomata H, Yamana T, Narazaki O, Kurokawa T. Ocular manifestations of congenital muscular dystrophy (Fukuyama type). Ann Ophthalmol 1983;15:921–923, 926–928.
4. Mishima H, Hirata H, Ono H, Choshi K, Nishi Y, Fukuda K. A Fukuyama type of congenital muscular dystrophy associated with atypical gyrate atrophy of the choroid and retina. A case report. Acta Ophthalmol (Copenh) 1985;63:155–159.
5. Ueda H, Gohdo T, Ohno S. Beta-dystroglycan localization in the photoreceptor and Muller cells in the rat retina revealed by immunoelectron microscopy. J Histochem Cytochem 1998;46:185–191.

Case of a Japanese Patient with X-linked Ocular Albinism Associated with the *GPR143* Gene Mutation

Albinism is an inherited disorder characterized by a reduction or absence of melanin in the hair, skin, and eyes. Albinism can be divided into two broad categories: oculocutaneous albinism and ocular albinism.[1] X-linked ocular albinism (XLOA) is characterized by nystagmus, decreased visual acuity, strabismus, fundus hypopigmentation, macular hypoplasia, and iris hypopigmentation with translucency. It is caused by mutations in the G protein-coupled receptor 143 (*GPR143*) gene (OMIM 300808), originally referred to as the *OA1* gene, which is located at Xp22.32.[2] The fundus of female carriers has a mosaic pattern of pigmentation and depigmentation, which helps in diagnosing XLOA.

We report on a Japanese boy with XLOA whose hair and skin appeared to be hypopigmented, causing some of the referring doctors and his parents to be concerned that he was suffering from oculocutaneous albinism. We detected a *GPR143/OA1* gene mutation, making this the first report of this mutation in Japan.

Case Report

The patient was a 4-month-old boy who had been born by normal delivery with a birth weight of 3148 g. His parents noticed that both his irides were blue and his eye movements appeared abnormal from birth. They consulted a pediatrician, who suspected oculocutaneous albinism. The patient was referred to us when he was 4 months old.

No family history of albinism was reported. His hair was mostly light brown, and his skin color was fair for a Japanese individual. He showed pendular horizontal nystagmus but could follow a slowly moving target. His refraction was –0.50 D = cyl –2.00 D Ax 180° (OD) and –0.50 D = cyl –1.50 D Ax 180° (OS). Slit-lamp examination showed that both irides were light brown (Fig. 1A, B). Bilateral foveal hypoplasia was present, and the ocular fundus was albinotic (Fig. 1C, D). Because his mother's fundus showed a mosaic pattern in the midperiphery, XLOA was diagnosed (Fig. 1E, F). He was also seen by a pediatrician of the Hamamatsu University School of Medicine, who diagnosed oculocutaneous albinism rather than ocular albinism (Fig. 1G, H). Because of the discrepancy in diagnoses, his parents wanted the diagnosis confirmed so as to know whether his skin needed to be protected from ultraviolet exposure.

After genetic counseling, the parents agreed to a genetic examination of their child and of themselves. The molecular genetics study was approved by the Institutional Review Board for Human Genetics and Genomic Research of Hamamatsu University School of Medicine. Nine exons and the surrounding regions of the *GPR143* gene were amplified by polymerase chain reaction (PCR) and directly sequenced. A splice mutation at the junction between exon 5 and intron 5, c.658+1G>A, was detected in the patient (Fig. 2). A heterozygous mutation was detected in his mother, but not in his father. The polymorphisms c.251–135C>T and c.767+10C>G were also detected in the patient.

Comments

This is the first report of a Japanese XLOA patient with a *GPR143* mutation. Various types of mutations in *GPR143* have been identified in Caucasian and Chinese populations. The splice mutation c.658+1G>A that we described here has been previously reported.[3]

Most Japanese patients with XLOA have brown irides that show no translucency, nonalbinotic fundi with moderate pigmentation, and normal skin and hair color.[4] However, the iris in our patient was light brown and the fundus was albinotic. His hair color was mostly light brown, and his skin color was fair for a Japanese individual. The skin and hair pigmentation in Caucasians with ocular albinism can be in the normal range but is frequently lighter in color than that of their siblings without XLOA. Recently, a Chinese family with XLOA and a *GPR143* mutation was reported to have iris hyperpigmentation.[5] Although the amount of pigment

Multiple keratocystic odontogenic tumors associated with nevoid basal cell carcinoma syndrome having distinct *PTCH1* mutations: a case report

Ryo Sasaki, DDS, PhD,[a] Toshiyuki Miyashita, MD, PhD,[b] Naoyuki Matsumoto, DDS, PhD,[c] Katsunori Fujii, MD, PhD,[d] Kayoko Saito, MD, PhD,[e] and Tomohiro Ando, DDS, PhD,[f]
Tokyo, Kahagawa, and Chiba, Japan
TOKYO WOMEN'S MEDICAL UNIVERSITY SCHOOL OF MEDICINE, KITASATO UNIVERSITY SCHOOL OF MEDICINE, NIHON UNIVERSITY SCHOOL OF DENTISTRY, AND CHIBA UNIVERSITY GRADUATE SCHOOL OF MEDICINE

Nevoid basal cell carcinoma syndrome (NBCCS) is a rare autosomal dominant disorder characterized by developmental abnormalities and a predisposition to cancers. Although multiple jaw tumors, such as keratocystic odontogenic tumors (KCOTs), are one of the most frequent complications in NBCCS, the molecular mechanism for how KCOTs develop in NBCCS is poorly understood. A 15-year-old girl with 2 jaw tumors was diagnosed as NBCCS according to the clinical criteria. The pathologic findings indicated that the 2 tumors were consistent with KCOTs. A *PTCH1* mutation, c.1472delT, was detected in her peripheral blood as well as in the 2 tumors. Interestingly, an additional *PTCH1* mutation, c.264_265insAATA, that was not present in the peripheral blood, was found in the maxillary tumor but not the mandibular tumor. The Ki-67 labeling index was significantly higher in the maxillary KCOT (17.7%) than in the mandibular KCOT (14.3%). These findings indicate distinct molecular mechanisms of tumorigenesis in these KCOTs. **(Oral Surg Oral Med Oral Pathol Oral Radiol Endod 2010;110: e41-e46)**

Nevoid basal cell carcinoma syndrome (NBCCS), or Gorlin syndrome, is an autosomal dominant disorder that was first described by Gorlin and Goltz in 1960.[1] It is characterized by developmental abnormalities such as bifid ribs and cleft lip and palate. It is also characterized by a high incidence of tumorigenesis, such as basal cell carcinoma and medulloblastoma. Palmar and plantar pits and calcification of the falx cerebri are also included as pathognomonic signs of NBCCS.[1-5] Its prevalences are estimated to range from 1 in 56,000 in the United Kingdom to 1 in 164,000 in Australia.[2,4] However, the prevalences remain unreported in other countries, including Japan.

The human homolog of *Drosophila patched*, *PTCH1*, which is mapped to the NBCCS locus on chromosome 9q22.3, was first reported to contain mutations in NBCCS patients in 1996.[6,7] Subsequently, 75% of Japanese NBCCS patients were found to have *PTCH* mutations.[8] Because the PTCH1 protein functions as a suppressive receptor for the secretory protein sonic hedgehog (SHH), the phenotypes of NBCCS are believed to develop based on constitutive activation of the SHH pathway.[9]

Multiple jaw cysts, which are currently termed keratocystic odontogenic tumors (KCOTs), can be the first signs of NBCCS.[10] The incidence of KCOTs in NBCCS ranges from 75% to 90%.[2-5] KCOTs, which were previously known as odontogenic keratocysts, are benign cystic lesions, but they often show locally destructive behaviors and high recurrence rates.[11] Therefore, KCOTs are defined as benign neoplasms of odontogenic origin in the World Health Organization classification revised in 2005.[12] However, the molecular mechanism for how KCOTs develop in NBCCS patients is poorly understood.

Supported in part by a Grant-in Aid for Research on Intractable Diseases from the Ministry of Health, Labor, and Welfare, Japan (no. H21-058), and by a Grant-in-Aid for Scientific Research from the Ministry of Education, Culture, Sports, Science, and Technology, Japan (no. 21591313).
[a]Assistant Professor, Department of Oral and Maxillofacial Surgery and Institute of Advanced Biomedical Engineering and Science, Tokyo Women's Medical University School of Medicine.
[b]Professor, Department of Molecular Genetics, Kitasato University School of Medicine.
[c]Assistant Professor, Department of Pathology, Nihon University School of Dentistry.
[d]Assistant Professor, Department of Pediatrics, Chiba University Graduate School of Medicine.
[e]Professor, Institute of Medical Genetics, Tokyo Women's Medical University School of Medicine.
[f]Professor, Department of Oral and Maxillofacial Surgery, Tokyo Women's Medical University School of Medicine.
Received for publication Feb 19, 2010; returned for revision Apr 1, 2010; accepted for publication Apr 5, 2010.
1079-2104/$ - see front matter

doi:10.1016/j.tripleo.2010.04.006

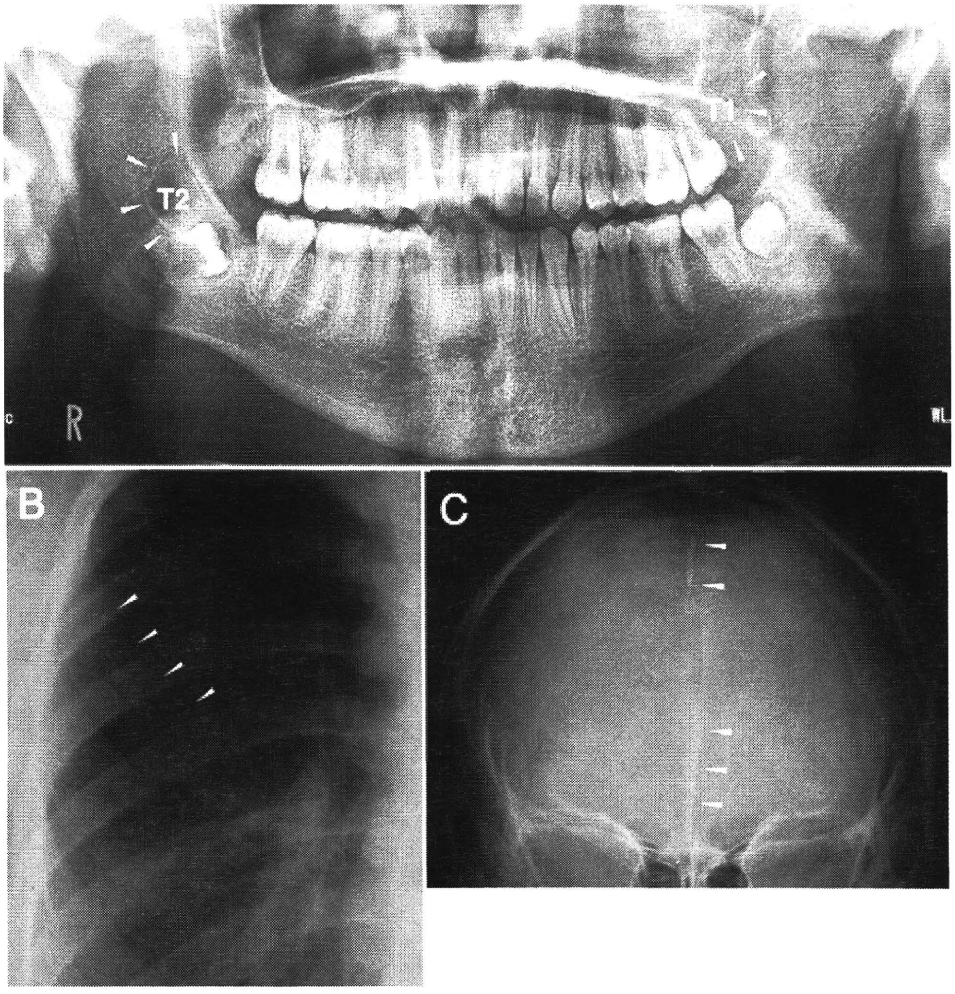

Fig. 1. X-ray images of the patient. **A,** Two jaw cysts (*arrowheads*) were detected in the maxilla (T1) and mandible (T2) in a panoramic x-ray image. **B and C,** Bifid ribs (*B*) and calcification of the falx cerebri (*C*) were also observed (*arrowheads*).

In the present study, we carried out a genetic analysis of the *PTCH1* gene to confirm the clinical diagnosis of NBCCS in a 15-year-old female patient. We also analyzed the *PTCH1* mutations in her KCOT tissues. As a result, an additional mutation was found in the maxillary KCOT but not in the mandibular KCOT. To investigate the effects of the presence or absence of this somatic mutation, we analyzed the expressions of prognostic molecular markers for KCOTs,[13-16] including Ki-67, cyclin D1, and p53, by immunohistochemistry.

CASE REPORT

A 15-year-old female patient was referred to our Department of Oral and Maxillofacial Surgery for 2 jaw cysts in the maxillary and mandibular regions, which were detected in a panoramic x-ray image taken by a local dental clinic (Fig. 1, *A*) that she attended because of pus discharge from the left maxillary gingiva. At 8 years of age, she had undergone a fenestration operation for a follicular cyst of the right mandibular cuspid in our department. After the operation, a panoramic x-ray image had shown no maxillary or mandibular cysts. She had no family history of NBCCS. She exhibited palmar pits, calcification of the falx cerebri, and bridging of the sella and bifid ribs (Fig. 1, *B* and *C*) and was clinically diagnosed with NBCCS according to the clinical criteria of Kimonis et al.[3] (Table I). Magnetic resonance imaging of the brain showed no evidence of medulloblastoma. She underwent 2 jaw cyst removals under general anesthesia. The pathologic findings of the maxillary and mandibular cysts indicated KCOTs. Genetic counseling and genetic testing were undertaken at the Institute of Medical Genetics, Tokyo Women's Medical University and Kitasato University. She had no tumor recurrences for >18 months after the surgery.

Mutational analysis

The study described below was approved by the Ethics Committee at Tokyo Women's Medical University and Kitasato University. After written informed consent was obtained, peripheral blood and tumor tissue samples were taken from

Table I. Clinical characteristics of the 15-year-old female patient according to the diagnostic criteria by Kimonis et al.[3]

Major Criteria	
>2 BCCs, or 1 BCC if <20 y	No
Odontogenic keratocysts of the jaw proven by histology	Yes
≥3 palmar or plantar pits	Yes
Bilamellar calcification of the falx cerebri	Yes
Bifid, fused, or markedly splayed ribs	Yes
First-degree relative with NBCCS	No
Minor Criteria	
Macrocephaly determined after adjustment for height	No
Congenital malformations	No
Other skeletal abnormalities	No
Radiologic abnormalities	Bridging of the sella turcica
Ovarian fibroma	No
Medulloblastoma	No

BCC, Basal cell carcinoma; *NBCCS,* nevoid basal cell carcinoma syndrome.

the patient. Genomic DNA was extracted using a QIAamp DNA Blood Midi Kit (Qiagen, Hilden, Germany). The genomic DNA samples were amplified with primers for all exons of the *PTCH1* gene as described previously.[8,10] The amplified products were gel-purified using a QIAex II Gel Extraction Kit (Qiagen) and cycle-sequenced with a BigDye Terminator v3.1 Cycle Sequencing Kit (Applied Biosystems, Foster City, CA) in both directions. The sequences were analyzed using a 3130 Genetic Analyzer (Applied Biosystems).

Immunohistochemistry

The KCOTs in the maxilla and mandible were compared for their expressions of prognostic factors for KCOTs, including Ki-67, cyclin D1, and p53.[13-16] Immunohistochemistry was performed on 10% neutral-buffered formalin-fixed and paraffin-embedded tissue sections. The tissue sections were deparaffinized in xylene and subjected to antigen retrieval by autoclaving (121°C, 2 atm, 15 min) in 0.01 mol/L citrate buffer (pH 6.0). After treatment with 3% hydrogen peroxide and a protein-blocking reagent (Dako, Glostrup, Denmark), the sections were incubated with primary antibodies against Ki-67 (clone MIB-1, 1:400 dilution; Dako), cyclin D1 (clone SP4, 1:250 dilution; Nichirei Bioscience, Tokyo, Japan), and p53 (clone DO-7, 1:300 dilution; Dako) at 4°C overnight. The sections were then incubated with a Dako Envision Kit (Dako), and antibody-antigen complexes were visualized by 3,3̀-diaminobenzidine staining. The sections were counterstained with Mayer hematoxylin and examined using a Leica DFC-6000B microscope system equipped with an ×40 objective lens (Leica Microsystems, Wetzlar, Germany). Digital images were captured with a CCD camera (DFC500; Leica Microsystems) and the numbers of Ki-67–, cyclin D1–, and p53-positive cells were counted in 5 randomly selected fields. The results were expressed as labeling indices (LI) for Ki-67, cyclin D1, and p53 as percentages of positive cells in the whole epithelial layer. The data are presented as mean ± SD. The significance of differences in the Ki-67, cyclin D1, and p53 LIs between the maxillary and mandibular tumors were analyzed by the Mann-Whitney *U* test. Values of $P < .05$ were considered to indicate statistical significance.

RESULTS

PTCH1 mutations in the peripheral blood and KCOTs

A *PTCH1* mutation, c.1472delT, was detected in the peripheral blood as well as in the 2 KCOTs in the maxilla and mandible. Moreover, an additional *PTCH1* mutation, c.264_265insAATA, was found in the maxillary KCOT but not in the peripheral blood or mandibular KCOT (Fig. 2; Table II).

Immunopositivities for Ki-67 and cyclin D1, but not p53, in the KCOTs

The pathologic findings indicated KCOTs with a lining of parakeratinized squamous epithelium without rete ridges in both the maxilla and the mandible. The columnar cells of each basal layer were often crowded. No apparent differences were found between the maxillary and mandibular tumors (Fig. 3, *A* and *B*).

It has been reported that the epithelial lining of KCOTs associated with NBCCS exhibits overexpression of Ki-67, p53, and cyclin D1.[15,17] Both the maxillary and the mandibular KCOTs showed frequent immunopositivities for Ki-67 and cyclin D1, but sparse p53 immunopositivity, in our patient (Fig. 3, *C-H*). The Ki-67 LI was significantly higher in the maxillary KCOT (17.7%) than in the mandibular KCOT (14.3%; $P < .05$). Although the cyclin D1 LI was higher in the maxillary KCOT (15.1%) than in the mandibular KCOT (13.6%), the difference was not significant ($P > .05$; Table III).

DISCUSSION

The *PTCH1* gene is considered to be a tumor suppressor gene, because heterozygous loss of *PTCH1* is detected in certain sporadic and familial cases of basal cell carcinoma.[18,19] Although Knudson's "2-hit" theory[20] was proposed as a pathogenesis for KCOTs associated with NBCCS,[21] the molecular mechanism for how KCOTs develop in NBCCS patients is poorly understood. There have been a small number of reports on mutational analyses of sporadic and NBCCS-associated KCOTs.[22,23] However, pairwise mutational analyses of both tumor and nontumor tissues or analyses of multiple KCOTs derived from a single patient have rarely been reported.

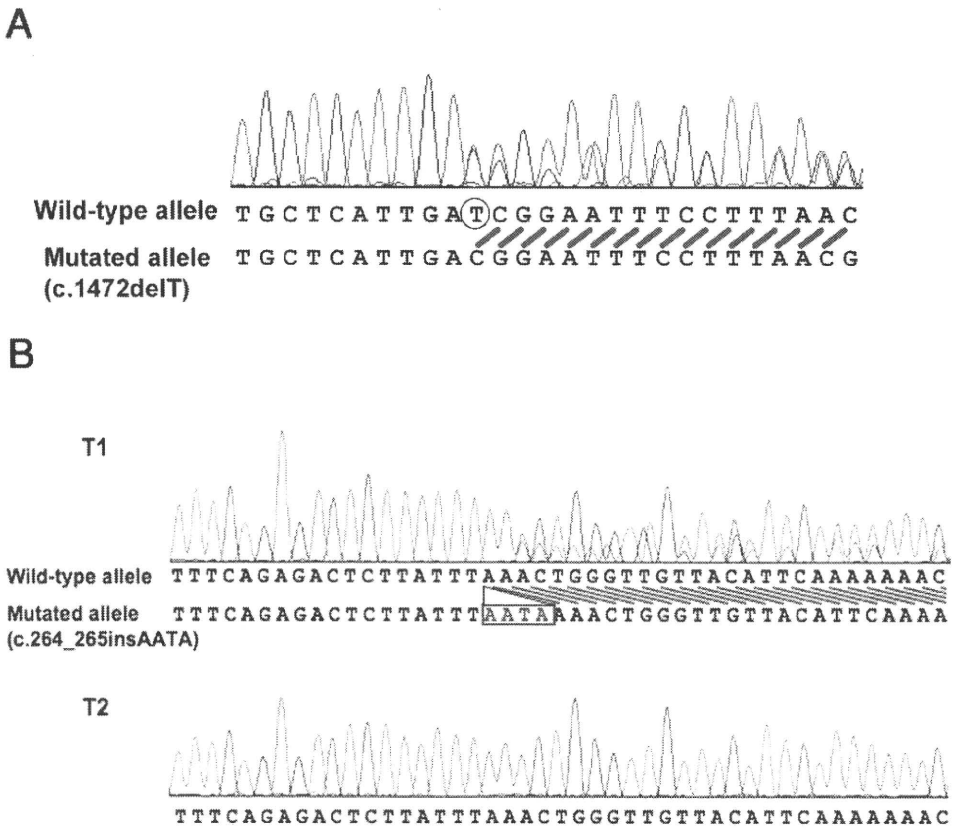

Fig. 2. Mutational analysis of the patient. **A,** A heterozygous deletion at nucleotide position 1472 of the *PTCH* gene (c.1472delT) is detected in the peripheral blood as well as in the 2 KCOTs removed from the maxilla and mandible. **B,** A heterozygous insertion between nucleotide positions 264 and 265 of the *PTCH1* gene (c.264_265insAATA) is detected in the maxillary tumor (T1). This mutation is not detected in the mandibular tumor (T2).

Table II. Summary of *PTCH1* mutation in peripheral blood and tumors

	Exon 2	*Exon 10*
Blood	—	c.1427delT
T1	c.264_265insAATA	c.1427delT
T2	—	c.1427delT

T1, Maxillary keratocystic odontogenic tumor; *T2,* mandibular keratocystic odontogenic tumor.

In the present study, we detected a germline mutation in a 15-year-old girl with NBCCS. Interestingly, an additional somatic mutation of a 4-bp insertion was found in the maxillary KCOT but not in the mandibular KCOT. It is unlikely that the absence of the additional mutation in the mandibular KCOT simply reflects the absence of tumor cells in the specimen, because both tumor samples contained similar amounts of KCOT cells. Since both mutations lead to truncation of the PTCH1 protein, which is deleterious for its function, the maxillary KCOT in this patient was thought to have developed because of complete loss of *PTCH1* function that resulted in constitutive activation of the SHH pathway. The mechanism for the tumor formation in the mandibular KCOT is currently unknown. Other components of the SHH pathway, such as *smoothened* and *suppressor of fused*, may be involved.[9] Nevertheless, it is intriguing that distinct somatic mutational events appear to be involved in the 2 tumors that developed simultaneously in this patient.

To address the question of whether the different somatic mutations led to different phenotypes in the 2 KCOTs, we performed immunohistochemical analyses of the tumors by using antibodies against proteins that are related to a poor prognosis for KCOTs.[13-16] Although the pathologic findings were similar between the 2 tumors, the LI of Ki-67, a proliferation marker, was significantly higher in the maxillary KCOT than in the mandibular KCOT. These observations are consistent with an earlier study in which *PTCH1* mutations were found to be related to epithelial cell proliferation in KCOTs.[24]

The p53 pathway was reported to synergize with the SHH pathway for the development of medulloblastoma

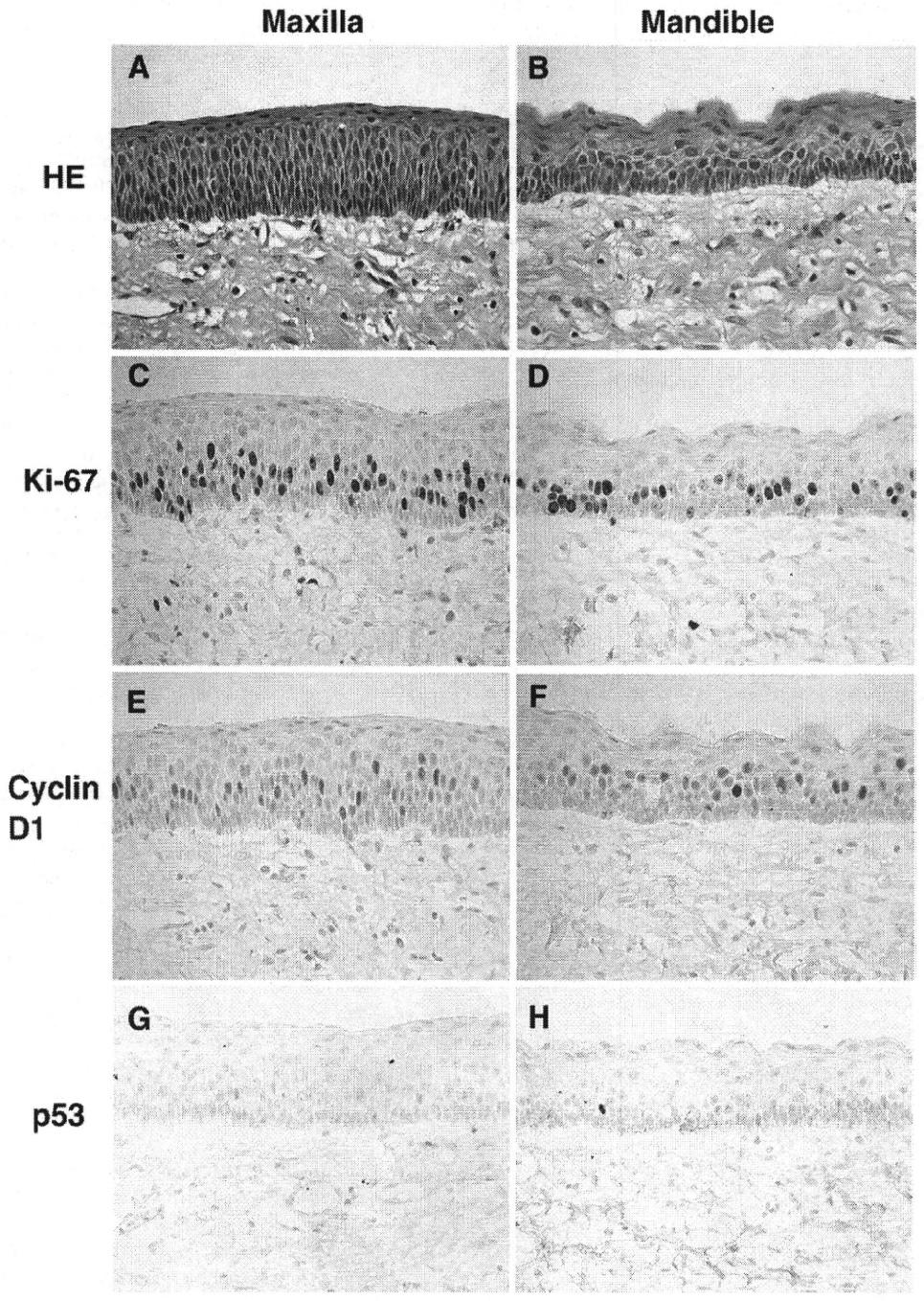

Fig. 3. Histopathologic features of the maxillary (**left**) and mandibular (**right**) keratocystic odontogenic tumors (KCOTs; magnification × 40). **A and B,** Hematoxylin-eosin (HE) staining shows a characteristic epithelial lining that is covered with parakeratinized squamous epithelium without rete ridges. **A,** Maxillary KCOT often exhibited crowded basal cell layer. **B,** KCOT with 6–8-cell layers, with palisaded basal cells. **C and D,** Ki-67–positive cells are stratified within basal and prickle cell layers. **E and F,** Cyclin D1–positive cells are mainly observed in the prickle cell layers. **G and H,** P53-positive cells are sparsely distributed.

associated with NBCCS in a mouse model, and p53 was also reported to be overexpressed in most NBCCS-associated KCOTs.[13,14,25] However, p53 staining was sparse in the samples from the present patient, indicating the absence of p53 mutations and suggesting that the p53 pathway was unlikely to be involved in this patient.

KCOTs were not considered to be tumors until recently. The accumulation of a spectrum of somatic and

Table III. Comparison of labeling indexes of keratocystic odontogenic tumors in maxilla and mandible

	Ki-67 (%)	*Cyclin D1 (%)*	*p53 (%)*
Maxilla	17.7 ± 3.9	14.3 ± 3.0	ND
Mandible	15.1 ± 3.2*	13.6 ± 1.4†	ND

Data are presented as mean ± SD and compared by unpaired *t* test.
ND, Not detected.
*$P < .05$ between maxilla and mandible.
†No significant difference between maxilla and mandible.

germline mutations in NBCCS-associated KCOTs is expected to help toward understanding the molecular pathogenesis of KCOTs.

The authors are indebted to the patient who participated in this study. They also thank Hiromi Hatsuse for excellent technical assistance.

REFERENCES

1. Gorlin RJ, Goltz RW. Multiple nevoid basal-cell epithelioma, jaw cysts and bifid rib. A syndrome. N Engl J Med 1960;262: 908-12.
2. Evans DGR, Ladusan EJ, Rimmer S, Burnell LD, Thakker N, Farndon PA. Complications of the nevoid basal cell carcinoma syndrome: results of the population based study. J Med Genet 1993;30:460-4.
3. Kimonis VE, Goldstein AM, Pastakia B, Yang ML, Kase R, DiGiovanna JJ, et al. Clinical manifestations in 105 persons with nevoid basal cell carcinoma syndrome. Am J Med Genet 1997;69:299-308.
4. Shanley S, Ratcliffe J, Hockey A, Haan E, Oley C, Ravine D, et al. Nevoid basal cell carcinoma syndrome: review of 118 affected individuals. Am J Med Genet 1994;50:282-90.
5. Ahn SG, Lim YS, Kim DK, Kim SG, Lee SH, Yoon JH. Nevoid basal cell carcinoma syndrome: a retrospective analysis of 33 affected Korean individuals. Int J Oral Maxillofac Surg 2004; 33:458-62.
6. Hahn H, Wicking C, Zaphiropoulous PG, Gailani MR, Shanley S, Chidambaram A, et al. Mutations of the human homolog of Drosophila patched in the nevoid basal cell carcinoma syndrome. Cell 1996;85:841-51.
7. Johnson RL, Rothman AL, Xie J, Goodrich LV, Bare JW, Bonifas JM, et al. Human homolog of patched, a candidate gene for the basal cell nevus syndrome. Science 1996;272:1668-71.
8. Fujii K, Kohno Y, Sugita K, Nakamura M, Moroi Y, Urabe K, et al. Mutations in the human homologue of *Drosophila patched* in Japanese nevoid basal cell carcinoma syndrome patients. Hum Mutat 2003;21:451-2.
9. Cohen MM. The hedgehog signaling network. Am J Med Genet 2003;123A:5-28.
10. Sasaki R, Saito K, Watanabe Y, Takayama Y, Fujii K, Agawa K, et al. Nevoid basal cell carcinoma syndrome with cleft lip and palate associated with the novel *PTCH* gene mutations. J Hum Genet 2009;54:7:398-402.
11. Morgan TA, Burton CC, Qian F. A retrospective review of treatment of the odontogenic keratocyst. J Oral Maxillofac Surg 2005;63:635-9.
12. Barnes L, Eveson JW, Reichart PA, Sidransky D, editors. World Health Organization classification of tumours. Pathology and genetics of head and neck tumours. Lyon: IARC Press; 2005. p. 306-7.
13. Ogden GR, Chisholm DM, Kiddie RA, Lane DP. P53 protein in odontogenic cysts: increased expression in some odontogenic keratocysts. J Clin Pathol 1992;45:1007-10.
14. Lombardi T, Odell EW, Morgan PR. P53 immunohistochemistry of odontogenic keratocysts in relation to recurrence, basal-cell budding and basal-cell naevus syndrome. Arch Oral Biol 1995; 40:1081-4.
15. Muzio LL, Staibano S, Pannone G, Bucci P, Nocini PR, Bucci E, et al. Expression of cell cycle and apoptosis-related proteins in sporadic odontogenic keratocysts and odontogenic keratocysts associated with the nevoid basal cell carcinoma syndrome. J Dent Res 1999;78:1345-53.
16. Kuroyanagi N, Sakuma H, Miyabe S, Machida J, A Kaetsu, M Yokoi, et al. Prognostic factors for keratocystic odontogenic tumor (odontogenic keratocyst): analysis of clinico-pathologic and immunohistochemical findings in cysts treated by enucleation. J Oral Pathol Med 2009;38:386-92.
17. Shear M. The aggressive nature of the odontogenic keratocyst: is it a benign cystic neoplasm? Part 2. Proliferation and genetic studies. Oral Oncol 2002;38:323-31.
18. Gailani MR, Stahle-Backdahl M, Leffell DJ, Glynn M, Zaphiropoulos PG, Pressman C, et al. The role of the human homologue of *Drosophila patched* in sporadic basal cell carcinomas. Nat Genet 1996;14:78-81.
19. Unden AB, Holmberg E, Lundh-Rozell B, Stahle-Backdahl M, Zaphiropoulos PG, Toftgard R, et al. Mutations in the human homologue of *Drosophila patched* (*PTCH*) in basal cell carcinomas and the Gorlin syndrome: different in vivo mechanisms of PTCH inactivation. Cancer Res 1996;56:4562-5.
20. Knudson AG. Mutation and cancer: statistical study of retinoblastoma. Proc Natl Acad Sci U S A 1971;68:823-30.
21. Levanat S, Gorlin RJ, Fallet S, Johnson DR, Fantasia JE, Bale AE. A two-hit model for defects in Gorlin syndrome. Nat Genet 1996;12:85-7.
22. Sun LS, Li XF, Li TJ. *PTCH1* and *SMO* gene alterations in keratocystic odontogenic tumors. J Dent Res 2008;87:575-9.
23. Pan S, Dong Q, Sun LS, Li TJ. Mechanisms of inactivation of *PTCH1* gene in nevoid basal cell carcinoma syndrome: modification of the two-hit hypothesis. Clin Cancer Res 2010;16: 442-50.
24. Pan S, Li TJ. *PTCH1* mutations in odontogenic keratocysts: are they related to epithelial cell proliferation? Oral Oncol 2009; 45:861-5.
25. Wetmore C, Eberhart DE, Curran T. Loss of p53 but not ARF accelerates medulloblastoma in mice heterozygous for patched. Cancer Res 2001;61:513-6.

Reprint requests:

Dr. Ryo Sasaki
Department of Oral and Maxillofacial Surgery
Tokyo Women's Medical University School of Medicine
8-1 Kawada-cho, Shinjuku-ku
Tokyo 162-8666
Japan
sasaki@oms.twmu.ac.jp

CLINICAL GENETICS
An International Journal of Genetics, Molecular, and Personalized Medicine

Clin Genet 2011: 79: 196–198
Printed in Singapore. All rights reserved

CLINICAL GENETICS
doi: 10.1111/j.1399-0004.2010.01527.x

Letter to the Editor

Entire *PTCH1* deletion is a common event in point mutation-negative cases with nevoid basal cell carcinoma syndrome in Japan

To the Editor:

Nevoid basal cell carcinoma syndrome [NBCCS (OMIM 109400)], also called Gorlin syndrome, is an autosomal dominant neurocutaneous disorder characterized by large body size, developmental and skeletal abnormalities, sensitivity to radiation, and an increased incidence of cancers such as basal cell carcinoma (BCC) and medulloblastoma (1). NBCCS is caused by inactivating mutations in the *Patched-1* (*PTCH1*) gene (2, 3). Heterozygous loss of *PTCH1* found in certain sporadic and familial cases of BCC indicates that *PTCH1* is also a tumor suppressor gene (4, 5).

Despite extensive efforts to detect mutations, they are still unidentified in 25–60% of patients (6–8). To date, we have analyzed 38 patients with NBCCS from 32 families. Eight of the families did not harbor any *PTCH1* mutations detectable by polymerase chain reaction (PCR)-based direct sequencing of the exons. To investigate the possibility of large deletions involving the *PTCH1* gene, we employed a high-resolution array-based comparative genomic hybridization technology. Consequently, we identified genomic deletions involving *PTCH1* in seven individuals from five of the eight point mutation-negative families (Fig. S1). These patients are listed in Table 1. Some of them have been reported previously by us (9) and one patient reported by others (NS6) (10) is also included in the table, all of which are of Japanese origin. To our knowledge, this table includes all the patients with *PTCH1* deletions in which the breakpoints have been identified at the nucleotide level. A schematic representation of each deletion's size together with the deleted genes is shown in Fig. 1a. Unlike in cases of Sotos syndrome and neurofibromatosis type 1, no recurrent breakpoints were observed in these patients (11, 12). Whereas deletions larger than 2.4 Mb were generated by non-homologous end joining, smaller ones (less than 1.2 Mb) were produced by *Alu*-mediated nonallelic homologous recombination (Fig. S2).

G19 and G36 inherited the deletion from their mothers (G27 and G43, respectively), whereas the deletion in NS6 is of paternal origin. The breakpoint sequences in these cases were completely conserved through generations. Other patients (G35, G10 and G5) did not have a family history of NBCCS and, therefore, the deletions seemed to be *de novo*. Patients harboring deletions of less than 2.4 Mb did not exhibit any phenotypes atypical for NBCCS despite that up to 22 RefSeq genes (four disease genes) were included in the deleted region. This implies that hemizygous loss of these genes, except for *PTCH1*, might not have an influence on any observable phenotypes. In contrast, deletions larger than 5.3 Mb led to phenotypes unusual for NBCCS including severe mental and motor retardation, epilepsy, and hypotonia (Table 1).

Interestingly, each *Alu*-mediated deletion was mediated by a distinct path of rearrangement (Fig. 1b). G36/43 had a crossing over point within the *Alu* elements generating a hybrid *Alu* element. In G19/27, however, the crossing over occurred near the poly-A tail of the proximal *Alu* element (9). Therefore, the proximal *Alu* remained intact while the distal *Alu* was deleted. In the third case, NS6, crossing over occurred at the 5′ end of the *Alu* elements and removed both *Alu* sequences leaving two short direct repeats flanking an *Alu* element on both sides called target-site duplications (10).

To date, we have analyzed 32 NBCCS families and identified entire deletions of *PTCH1* in 5 families. This implies that 16% of NBCCS families (five of the eight point mutation-negative families) can be explained by the entire loss of *PTCH1*. Mutations are not observed in the *PTCH1*-coding sequences in considerable numbers of NBCCS cases not only in Japanese but also in other ethnicities and, apart from *PTCH1*, only one *PTCH2* and one *SUFU* mutation in NBCCS have been

Table 1. NBCCS patients with gene deletions

Patient No.	Age (years)	Size	Deleted nucleotide No.[a]	Deleted RefSeq genes[b]	Deleted disease genes[b]	Predicted mechanism of deletion	Atypical phenotypes
G19[c]	10	165 kb	97,187,146–197,350,058	1	1	Alu-mediated NAHR[d]	None
G27[e]	40	165 kb	97,187,146–97,350,058	1	1	Alu-mediated NAHR	None
G36	8 M[f]	1.1 Mb	96,766,985–97,885,391	9	2	Alu-mediated NAHR	None
G43[g]	32	1.1 Mb	96,766,985–97,885,391	9	2	Alu-mediated NAHR	None
NS6[h]	NA[i]	1.2 Mb	96,070,054–97,646,323[j]	13	3	Alu-mediated NAHR	None
G35	5	2.4 Mb	95,880,121–98,238,462	22	4	NHEJ[k] with 2-bp overlap	None
G10[c]	8	5.3 Mb	94,898,311–100,101,915	58	6	NHEJ with 1-bp overlap	severe mental and motor retardation, epilepsy, hypotonia, inguinal hernia
G5[c]	12	11 Mb	90,617,332–101,647,101	93	13	NHEJ with 7-bp addition	severe mental and motor retardation, epilepsy, hypotonia, webbed neck, hydronephrosis

[a]Nucleotide numbers are based on UCSC Genome Browser on Human March 2006 Assembly (hg18).
[b]Numbers of the deleted genes are based on Database of Genomic variants (http://projects.tcag.ca/variation/).
[c]Fujii et al. 2007 (9).
[d]nonallelic homologous recombination.
[e]G19's mother.
[f]8 months.
[g]G36's mother.
[h]Takahashi et al. 2009 (10).
[i]Not available.
[j]Distal breakpoint is ambiguous due to the complicated structure of the deletion (10).
[k]non-homologous end joining.

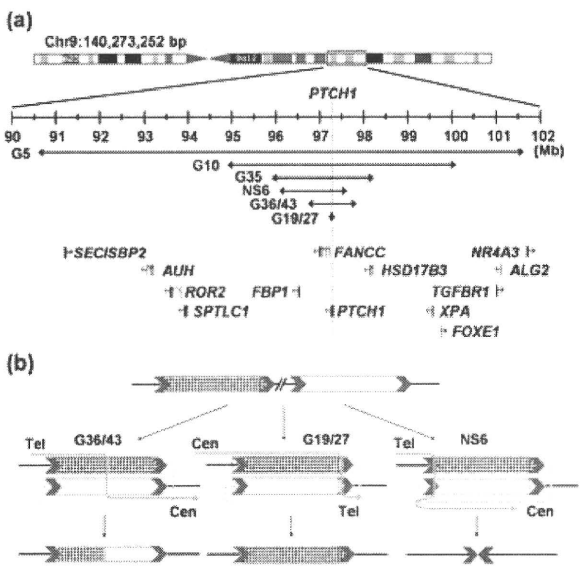

Fig. 1. Schematic representation of the deletions. (**a**) Architecture of the deleted region. Horizontal arrows represent the deleted regions in the six families listed in Table 1. Disease genes are depicted at the bottom. Vertical dotted lines indicate the positions of *PTCH1*. (**b**) Three different types of recombination between *Alu* elements observed in NBCCS patients. Black and gray lines represent flanking and intervening regions, respectively. Curved red arrows show the paths of recombination events. Red and blue arrowheads represent target-site duplications (TSDs) of the two elements, respectively. Cen, centromeric; Tel, telomeric.

reported (13, 14). Therefore, it is strongly advisable to investigate the possibility of the gene deletion in point mutation-negative cases.

Supporting Information

The following Supporting information is available for this article:

Fig. S1. Microarray profile of two individuals with a copy number loss at 9q22. Probes are ordered on the x-axis according to physical mapping positions. Test over reference signal intensity ratios for each probe are given on the y axis. For clarity, data are smoothed over a 50-probe window. The position of *PTCH1* is indicated by a vertical dotted line. Disease genes lying in this region are schematically indicated at the bottom.

Fig. S2. DNA sequence of junction fragments. The DNA sequence for each deletion-specific junction fragment obtained by polymerase chain reaction (PCR) was aligned to the wild-type flanking genome sequence for both proximal and distal breakpoints. Alignments with the proximal boundary are shaded in light gray, and those with the distal boundary in dark gray. The estimated cross over points are shaded in red. (A) Sequence alignment in G36/43. Red lines surround *Alu* sequences. The precise length of polyT could not be determined due to the heterogeneity of the PCR product (A_{20-22}). (B) Sequence alignment in G35.

Additional Supporting information may be found in the online version of this article.

Please note: Wiley-Blackwell Publishing is not responsible for the content or functionality of any supplementary materials supplied by the authors. Any queries (other than missing material) should be directed to the corresponding author for the article.

Acknowledgements

We thank all patients, their families and collaborating doctors for participating in this study. We are also grateful to Noriko Ito for technical support. This work was partly supported by a Grant-in-Aid for Research on Intractable Diseases from the Ministry of Health, Labor and Welfare, Japan (No. H22-120), and by a Grant-in-Aid for Scientific Research (C) from the Ministry of Education, Culture, Sports, Science and Technology, Japan (No. 21591313).

K Nagao[a]
K Fujii[b]
K Saito[c]
K Sugita[d]
M Endo[b]
T Motojima[e]
H Hatsuse[a]
T Miyashita[a]
[a]Department of Molecular Genetics, Kitasato University School of Medicine, Sagamihara, Japan,
[b]Department of Pediatrics, Chiba University Graduate School of Medicine, Chiba, Japan,
[c]Institute of Medical Genetics, Tokyo Women's Medical University, Tokyo, Japan,
[d]Division of Child Health, Faculty of Education, Chiba University, Chiba, Japan, and
[e]Department of Pediatrics, Motojima General Hospital, Ota, Japan

References

1. Gorlin RJ. Nevoid basal-cell carcinoma syndrome. Medicine (Baltimore) 1987: 66: 98–113.
2. Johnson RL, Rothman AL, Xie J et al. Human homolog of *patched*, a candidate gene for the basal cell nevus syndrome. Science 1996: 272: 1668–1671.
3. Hahn H, Wicking C, Zaphiropoulous PG et al. Mutations of the human homolog of Drosophila *patched* in the nevoid basal cell carcinoma syndrome. Cell 1996: 85: 841–851.
4. Gailani MR, Stahle-Backdahl M, Leffell DJ et al. The role of the human homologue of *Drosophila patched* in sporadic basal cell carcinomas. Nat Genet 1996: 14: 78–81.
5. Unden AB, Holmberg E, Lundh-Rozell B et al. Mutations in the human homologue of *Drosophila patched* (*PTCH*) in basal cell carcinomas and the Gorlin syndrome: different *in vivo* mechanisms of *PTCH* inactivation. Cancer Res 1996: 56: 4562–4565.
6. Fujii K, Kohno Y, Sugita K et al. Mutations in the human homologue of *Drosophila patched* in Japanese nevoid basal cell carcinoma syndrome patients. Hum Mutat 2003: 21: 451–452.
7. Marsh A, Wicking C, Wainwright B, Chenevix-Trench G. DHPLC analysis of patients with Nevoid Basal Cell Carcinoma Syndrome reveals novel *PTCH* missense mutations in the sterol-sensing domain. Hum Mutat 2005: 26: 283.
8. Lindström E, Shimokawa T, Toftgård R, Zaphiropoulos PG. PTCH mutations: distribution and analyses. Hum Mutat 2006: 27: 215–219.
9. Fujii K, Ishikawa S, Uchikawa H et al. High-density oligonucleotide array with sub-kilobase resolution reveals breakpoint information of submicroscopic deletions in nevoid basal cell carcinoma syndrome. Hum Genet 2007: 122: 459–466.
10. Takahashi C, Kanazawa N, Yoshikawa Y et al. Germline *PTCH1* mutations in Japanese basal cell nevus syndrome patients. J Hum Genet 2009: 54: 403–408.
11. Kurotaki N, Harada N, Shimokawa O et al. Fifty microdeletions among 112 cases of Sotos syndrome: low copy repeats possibly mediate the common deletion. Hum Mutat 2003: 22: 378–387.
12. Dorschner MO, Sybert VP, Weaver M, Pletcher BA, Stephens K. *NF1* microdeletion breakpoints are clustered at flanking repetitive sequences. Hum Mol Genet 2000: 9: 35–46.
13. Fan Z, Li J, Du J et al. A missense mutation in *PTCH2* underlies dominantly inherited NBCCS in a Chinese family. J Med Genet 2008: 45: 303–308.
14. Pastorino L, Ghiorzo P, Nasti S et al. Identification of a *SUFU* germline mutation in a family with Gorlin syndrome. Am J Med Genet A 2009: 149A: 1539–1543.

Correspondence:
Toshiyuki Miyashita, MD, PhD
Department of Molecular Genetics
Graduate School of Medical Science
Kitasato University
1-15-1 Kitasato
Minami-ku
Sagamihara 252-0374
Japan
Tel.: +81 42 778 8816
Fax: +81 42 778 9214
e-mail: tmiyashi@med.kitasato-u.ac.jp

脊髄性筋萎縮症

斎藤加代子　伊藤万由里　荒川玲子　東京女子医科大学附属遺伝子医療センター

はじめに

脊髄性筋萎縮症(SMA)は脊髄の前角細胞の変性による筋萎縮と進行性筋力低下を特徴とする常染色体劣性遺伝病である．SMAの遺伝子同定のためには明確な診断基準と分類を確立することが必要であるという考えのもとに，国際SMA協会が組織され，図1に示す診断基準が作成された[1]．さらに2009年にはわが国の厚生労働科学研究費補助金(難治性疾患克服研究事業)神経変性疾患に関する調査研究班において図2のような診断基準が作成された[2]．

従来，広義の脊髄性進行性筋萎縮症(SPMA)として，小児期発症のSMAと成人発症のSPMAを総称してSPMAとしており，わが国の難治性疾患克服研究事業において，SPMAの疾患名が使用されていた．海外の成書や論文では，「広義のSPMA」という表現は使用されておらず，「広義のSMA」として表わされている．さらに，ICD-10では，「G-12：脊髄性筋萎縮症及び関連症候群」のなかに，G-122：脊髄性進行性筋萎縮症，G-129脊髄性筋萎縮症が含まれている．そこで2009年に国際的な表現に統一を図るため，「脊髄性筋萎縮症(SMA)」となった．

小児期特に乳幼児期発症のSMAの多くはsurvivial motor neuron (SMN)遺伝子に変異を示すSMAであり，成人発症例や図1の除外項目に当てはまるような所見を示す場合，遺伝子的に異質である可能性が高い．本稿では遺伝子診断が可能であるSMAとして，SMN遺伝子に変異を示すSMAを中心として述べる．

■図1　脊髄性筋萎縮症の診断基準

包含項目	除外項目
Ⅰ．筋力低下 対称性 近位筋＞遠位筋 下肢＞上肢 躯幹および四肢 Ⅱ．脱神経 舌の線維束性収縮 手の振戦 筋生検ー萎縮筋線維の群 筋電図ー神経原性変化	1. 中枢神経機能障害 2. 関節拘縮症 3. 外眼筋，横隔膜，心筋の障害，聴覚障害，著しい顔面筋罹患 4. 知覚障害 5. 血清CK値＞正常上限の10倍 6. 運動神経伝導速度＜正常下限の70% 7. 知覚神経活動電位の異常

(国際SMA協会報告，1992)

■図2　脊髄性筋萎縮症の特定疾患診断基準

1．主要項目
(1)臨床所見
①下記のような下位運動ニューロン症候を認める．
筋力低下
筋萎縮
舌，手指の線維束性収縮 fasciculation
腱反射は減弱から消失
②下記のような上位運動ニューロン症候は認めない．
痙縮
腱反射亢進
病的反射陽性
③経過は進行性である．
(2)臨床検査所見
筋電図で高振幅電位や多相性電位等の神経原性所見を認める．
(3)遺伝子診断
survival motor neuron (SMN) 遺伝子変異を認める．
2．鑑別診断
(1)　筋萎縮性側索硬化症
(2)　球脊髄性筋萎縮症
(3)　脳腫瘍・脊髄疾患
(4)　頸椎症，椎間板ヘルニア，脳および脊髄腫瘍，脊髄空洞症等
(5)　末梢神経疾患
(6)　多発性神経炎(遺伝性，非遺伝性)，多発限局性運動性末梢神経炎 multifocal motor neuropathy 等
(7)　筋疾患：筋ジストロフィー，多発筋炎等
(8)　感染症に関連した下位運動ニューロン障害：ポリオ後症候群等
(9)　傍腫瘍症候群
(10)　先天性多発性関節拘縮症
(11)　神経筋接合部疾患
3．診断の判定
上記1の(1)①②③すべてと(2)，(3)の1項目以上を満たし，かつ2のいずれでもない．

(厚生労働省神経変性疾患調査研究班(中野今治班長)，2009)